JOURNAL OF COMPUTATIONAL PHYSICS 5, 487–506 (1970)

Numerical Analysis of Viscous One-Dimensional Flows*

GINO MORETTI† AND MANUEL D. SALAS‡

Polytechnic Institute of Brooklyn, Farmingdale, New York 11735

Received November 11, 1969

The flow of a viscous, heat-conducting gas produced by an accelerating piston is analyzed numerically. The formation of a shock in a viscous flow is studied. A discussion of accuracy and practicality of a numerical analysis of the problem is given. It is concluded that, although very accurate results may be obtained, in principle, regardless of the Reynolds number of the flow, the assumption of a shock as a sharp discontinuity is the only practical way to handle flows whose Reynolds number per unit length is higher than 100.

I. REAL AND ARTIFICIAL VISCOSITY FROM A NUMERICAL STANDPOINT

Time-dependent computational techniques for inviscid flows have been the subject of a great number of papers. After more than a decade of studies and experimentations, it is clear that such techniques can work very well so long as the flow is continuous. However, in problems of practical interest discontinuities exist and are the most relevant features of the flow. The techniques mentioned above may work for a flow containing discontinuities only if these are smeared out artificially and replaced by a fast but smooth transition over several mesh intervals. Such an effect is obtained if the numerical scheme in finite difference form differs from the partial differential equations of inviscid flow for the presence of terms which can be interpreted as representing an artificial viscosity. Whether acknowledged or not, artificial viscosity is present in all computations of inviscid flows where discontinuities are smeared out.

In previous papers [1, 2], an attempt has been made to show the inconveniences of using artificial viscosity, and a typical one-dimensional problem has been studied to prove that numerical computations of inviscid flows with discontinuities can be performed without artificial viscosity, provided that the discontinuities are properly treated.

* This research was conducted under the sponsorship of the Office of Naval Research under Contract No. Nonr 839(34), Project No. NR 061-135.

† Professor of Aerospace Engineering.

‡ NDEA Graduate Fellow.

581/5/3-9

If the flow itself is viscous, all discontinuities are naturally smeared out. It should, then, be possible to solve problems numerically by using a finite-difference scheme consistent with the Navier–Stokes equations and not containing artificial viscosity. Three questions must be answered, however, before attempting general applications of a numerical scheme:

(1) Is it possible to use natural viscosity to smear out discontinuities in a numerical computation, obtaining the same effects as in the natural flow? In other words, is it possible to obtain numerically a good description of the structure of a shock wave?

(2) If the shock wave is too thin, and no artificial viscosity is used, are the results of a viscous computation as bad as those of an inviscid computation where no proper treatment is given to the discontinuity [2], and what should be done in this case?

(3) Is, by any chance, artificial viscosity concealed in the numerical scheme and defacing the effects of natural viscosity? In other words, to what extent can one make sure that the numerical results depend on the actual Reynolds number of the flow, not on a fictitious Reynolds number due to artificial viscosity?

The present paper is an attempt to answer such questions in a simple case. The results, however, can be easily extended to more complicated cases.

II. The Piston-Driven One-Dimensional Viscous Flow

A study is made of the viscous, one-dimensional flow produced by a piston starting from rest and accelerating until it reaches a certain speed; then, the piston proceeds at a constant speed. This problem has been chosen, instead of the problem, considered by other authors, of a viscous shock separating two regions of uniform flow, for three reasons:

(1) The present problem is physically more realistic (it does not represent the collapse of a discontinuity, which cannot exist physically, but rather the formation of a fast transition, which is a physical fact),

(2) Consequently, we have a way of testing whether an alleged time-dependent technique actually depicts a physical phenomenon which takes place in time,

(3) The numerical analysis of the transient shows very clearly how certain features appear which hamper the numerical analysis of the steady flow. By understanding their causes, one can be guided to find out proper remedies.

In the course of this analysis, we will frequently make reference to the inviscid flow problem having the same initial conditions and the same piston path. As long

as no shock is formed, an exact solution of the inviscid problem is available in closed form. This and the numerical solution extended to times following the formation of a shock are presented in detail in [2].

III. Equations of Motion

The Navier–Stokes equations of motion are written in a nondimensional form. Pressure and density in the gas at rest are taken as unity, and $P = \ln p$. Nondimensional temperature and entropy are $\mathscr{T} = p/\rho$ and $S = P - \gamma \ln \rho$ where γ is the ratio of specific heats. The reference velocity, u_{ref}, is the speed of sound of the gas at rest divided by $\sqrt{\gamma}$. The unit of length, x_{ref}, is arbitrary and the unit of time is $t_{\text{ref}} = x_{\text{ref}}/u_{\text{ref}}$. A Reynolds number per unit length is defined by density, viscosity, and speed of sound of the gas at rest. If the relation

$$\mu = .35 \sqrt{\frac{8}{\gamma\pi}}\, a\rho\lambda$$

between viscosity and the molecular mean free path, λ, is accepted (where the quantities have physical dimensions), it follows that

$$\lambda = \frac{2.12}{\rho\sqrt{\mathscr{T}}} \frac{1}{\text{Re}} \tag{1}$$

in nondimensional form.

In this paper the viscosity will be assumed as constant. Consequently, the Navier–Stokes equations are, in matrix form:

$$f_t + Bf_x + g = 0 \tag{2}$$

where subscripts mean partial differentiations and

$$f = \begin{bmatrix} P \\ u \\ S \end{bmatrix}, \qquad B = \begin{bmatrix} u & \gamma & 0 \\ \mathscr{T} & u & 0 \\ 0 & 0 & u \end{bmatrix}, \qquad g = \begin{bmatrix} V_2 \\ V_1 \\ V_2 \end{bmatrix}$$

$$V_1 = c_1 u_{xx}\mathscr{T}/p, \qquad V_2 = (c_2 u_x{}^2 + c_3 \mathscr{T}_{xx})/p \tag{3}$$

$$c_1 = -\frac{4}{3}\frac{\sqrt{\gamma}}{\text{Re}}, \qquad c_2 = (\gamma - 1)\, c_1, \qquad c_3 = -\frac{\gamma\sqrt{\gamma}}{\text{Re Pr}}$$

and Pr is the Prandtl number.

IV. A First Numerical Scheme Using an Evenly Spaced Mesh

The equations of motion (2) are solved approximately by a numerical technique of second order accuracy. First, we attack the problem in a simple way, by using an evenly spaced distribution of nodal points along the x-axis.

Let $b = b(t)$ be the abscissa of the driving piston. The following change of coordinates is made:

$$\begin{aligned} X &= x - b(t) \\ T &= t. \end{aligned} \tag{4}$$

The transformed equations of motion are:

$$f_T + Af_X + g = 0 \tag{5}$$

where

$$A = \begin{bmatrix} C & \gamma & 0 \\ \mathscr{T} & C & 0 \\ 0 & 0 & C \end{bmatrix}, \qquad C = u - \dot{b}, \qquad g = \begin{bmatrix} V_2 \\ V_1 \\ V_2 \end{bmatrix} \tag{6}$$

$$V_1 = c_1 u_{XX} \mathscr{T}/p, \qquad V_2 = (c_2 u_X{}^2 + c_3 \mathscr{T}_{XX})/p$$

The values of f at $T + \Delta T$ are obtained from the values of f at T by the rule:

$$f(T + \Delta T) = f(T) + f_T \Delta T + \tfrac{1}{2} f_{TT} \Delta T^2 \tag{7}$$

The values of f_T are computed at T by (5). The X-derivatives in (5) are replaced by centered differences; the values of g are also computed using centered differences, and stored. To compute f_{TT}, we differentiate (5) with respect to X and then with respect to T, obtaining

$$\begin{aligned} f_{TX} &= f_{TX}^{(1)} + f_{TX}^{(2)} \\ f_{TX}^{(1)} &= -(A_X f_X + A f_{XX}), \qquad f_{TX}^{(2)} = -g_X \end{aligned} \tag{8}$$

and a similar expression for f_{TT}.

The splitting of f_{TX} and f_{TT} into two parts is necessary to avoid recomputation of derivatives in the numerical scheme. First, $f_{TX}^{(1)}$ is evaluated, by using the equations

$$A_X = \begin{bmatrix} C_X & 0 & 0 \\ \mathscr{T}_X & C_X & 0 \\ 0 & 0 & C_X \end{bmatrix}, \qquad C_X = u_X, \qquad \mathscr{T}_X = \mathscr{T}\left(\frac{\gamma - 1}{\gamma} P_X + \frac{1}{\gamma} S_X\right) \tag{9}$$

and replacing the X-derivatives by centered differences. Then $f_{TT}^{(1)}$ is evaluated, in a similar way.

In this connection, the values of u_T, P_T, and S_T computed above are used. The values of g_T are obtained by taking backward differences of the values of g at T and $T - \Delta T$. The values of g_X are obtained approximately out of centered differences of the values of g computed previously.

At the right boundary, located at a distance x_0 from the piston, P, u, and S are assumed equal to zero. The piston point is treated as if the flow were only slightly perturbed by viscosity. Equations (2) are recast in characteristic form and the equation

$$aP' - \gamma u' = -aV_2 + \gamma V_1 \tag{10}$$

where $'$ denotes differentiation with respect to time along the characteristic defined by

$$\frac{dx}{dt} = u - a \tag{11}$$

is used. For a point on the piston at time $t + \Delta t$, the initial point on the characteristic at time t has the abscissa

$$x_* = b(t + \Delta t) - (u - a)\,\Delta t \tag{12}$$

where u and a are averaged along the segment of characteristic. Since u at the piston is known, (10) allows us to compute P at the piston. The right-hand side of the equation is considered constant along the segment of characteristic and taken equal to its value at x_*.

The entropy is obtained by integrating

$$\frac{DS}{Dt} = -V_2 \tag{13}$$

between times t and $t + \Delta t$.

At this stage, all the information necessary for the code is available, except the time step size. It is well-known that explicit integration schemes such as the one described above are only conditionally stable. In many cases the scheme may be unconditionally unstable. Criteria for determining the maximum time step size which can be used without generating instability have been established for various schemes but only for linear problems, generally with constant coefficients. The present scheme contains too many nonlinear effects and a criterion based on a drastic linearization of the scheme might be unrealistic. We have decided not to search for it. The labor involved, even after linearizing the equations, would still be too great. No closed form solution could be obtained. The eigenvalues of the growth matrix could be obtained only numerically and too many parameters are involved.

We prefer to resort to qualitative arguments and some experiments. In the absence of viscous terms, the Courant–Friedrichs–Lewy rule [3] can be applied:

$$\Delta t \leqslant \frac{\Delta x}{\max(|u| + a)} \tag{14}$$

This means that the domain of dependence of the node to be computed must be wider than its domain of dependence as defined by the partial differential equations (that is, by the two characteristic lines converging to the node). The viscous terms have a diffusive effect; as long as the Reynolds number is high, the characteristics tend to be smeared out. Consequently, the domain of dependence of a node gets wider, and the right-hand side of (14) should be affected by a factor, less than 1, and decreasing with the Reynolds number. In its crudity, the above argument reminds one of a more elaborate discussion available in the open literature [6]. Obviously, if the Reynolds number becomes too small, the viscous terms eventually become more important than the inviscid terms; the physical meaning of the characteristics is lost and consequently a criterion based on a modification of (14) is meaningless.

By numerical experimentation we found that, if

$$\Delta t = \epsilon \frac{\Delta x}{\max(|u| + a)} \tag{15}$$

is used instead of (14), the maximum value acceptable for ϵ without infringing stability is given by Fig. 1.

In conclusion, a lower Reynolds number entails a lower $\Delta t/\Delta x$ ratio. It is interesting to note that, if the Reynolds number is low, Δx itself can be chosen fairly

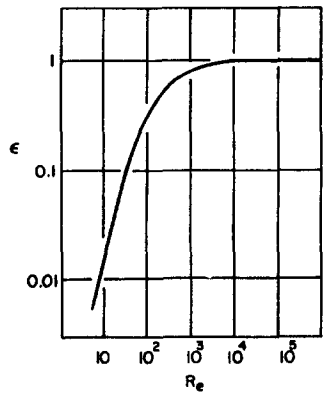

FIG. 1. Stability parameter vs. Reynolds number.

large. If the Reynolds number grows, $\Delta t/\Delta x$ can grow but Δx must be made smaller and smaller. We are going to analyze the problem of the space mesh size in greater detail in what follows.

V. Discussion of Some Numerical Results

We present the result of computations made with the scheme described above in three cases. In all of them the piston path is defined by

$$b(t) = \begin{cases} t^2 & (0 \leqslant t \leqslant .7395) \\ 1.479t - .54696025 & (t \geqslant .7395) \end{cases} \tag{16}$$

The piston path is so chosen that, if the flow were inviscid, the Mach number of the shock would be equal to 2 once a steady state has been reached.

In [2], it has been shown that a steady state is indeed reached for an inviscid flow, in a relatively short time. See Fig. 2, where some plots of $u(x)$ are shown, at various values of t, as they result from a numerical computation. The steady state is practically well-established at $t = 1.5$.

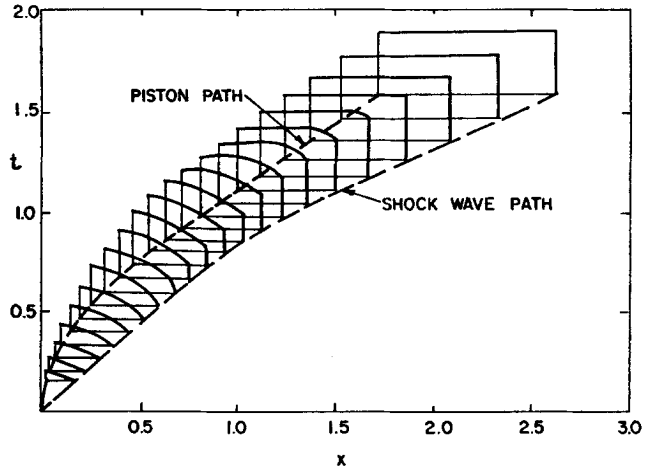

Fig. 2. Velocity distribution in the inviscid flow induced by an accelerating piston.

Table I shows the values of the Reynolds numbers in each of the three cases, together with some information about mesh size, step size, and other data of administrative interest. The Prandtl number is always assumed equal to $\frac{3}{4}$. The mean free path is computed from (1), assuming the values of ρ and T on the high

TABLE I

Case No	Re	x_0	λ	Δx	ϵ	N	K	t_0	t_c	t_{ref}	$\tilde{t}_0$	τ
1	10	2.	0.05	0.04	0.02	51	6600	1.980	129.6″	0.66	1.31	99
2	100	1.	0.005	0.02	0.25	51	600	1.2	14.15″	6.6×10^{-2}	7.2×10^{-2}	179
3	1000	1.	0.0005	0.01	0.4	101	599	1.0	26.7″	6.6×10^{-3}	6.6×10^{-3}	4045

N = total number of nodes
K = total number of steps
t_0 = value of t at which the computation was stopped
t_c = real computational time (on a CDC 6600 computer)
x_0 = width of the computed region
$x_{ref} = 1$ cm, $\gamma = 1.4$,
$\mu/\rho_0 = 0.18$ cm²/sec
$\tilde{t}_0(\text{sec}) = t_0 t_{ref}$
$\tau = t_c/\tilde{t}_0$ = ratio between computational time and real time

pressure side of the shock, after the shock Mach number has reached its steady value, $M = 2$.

Plots of $u(x)$ at various values of t are reported in Figs. 3, 4 and 5. One can see that the u-distributions at Re = 10 are substantially different from the inviscid case. The perturbation is spread over a region much wider than the region defined by the piston and the characteristic issuing from the origin (the broken line in the figure) where all motion is confined in the inviscid case. The steepening of the u-distribution

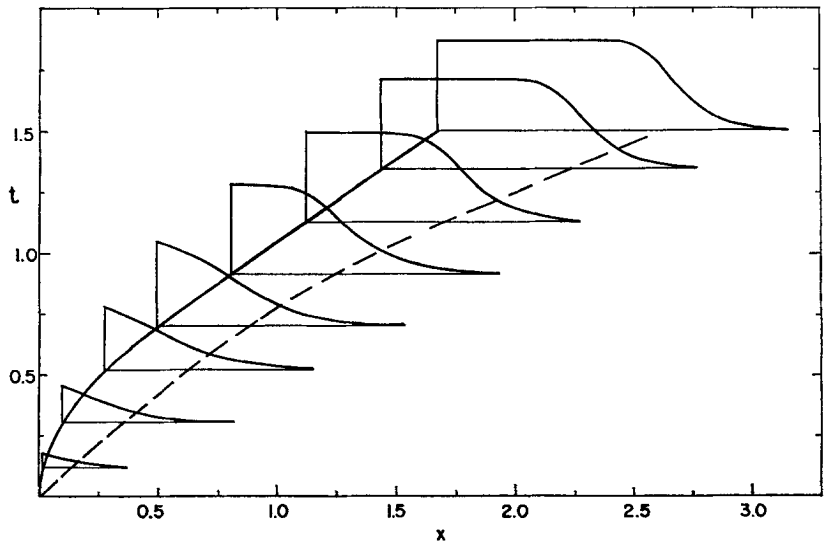

FIG. 3. Velocity distribution, viscous flow, Re = 10. Results obtained by using a constant mesh size.

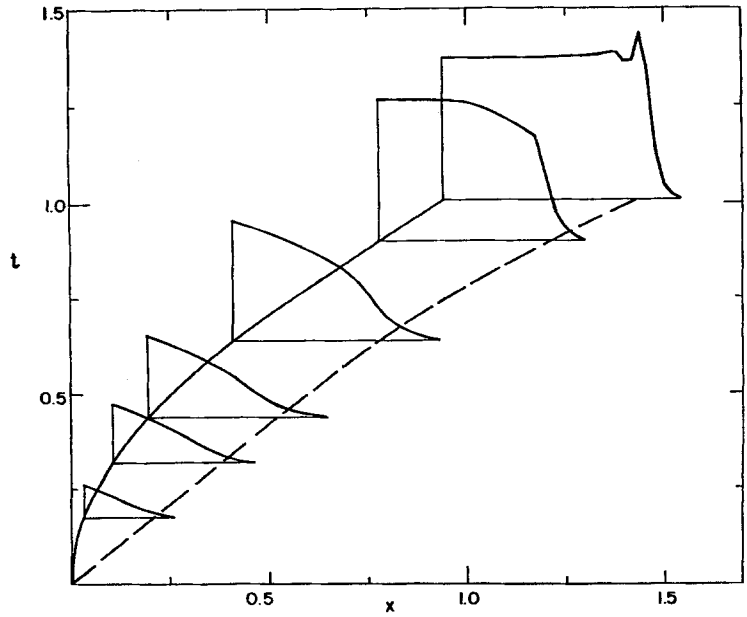

FIG. 4. Velocity distribution, viscous flow, Re = 100. Results obtained by using a constant mesh size.

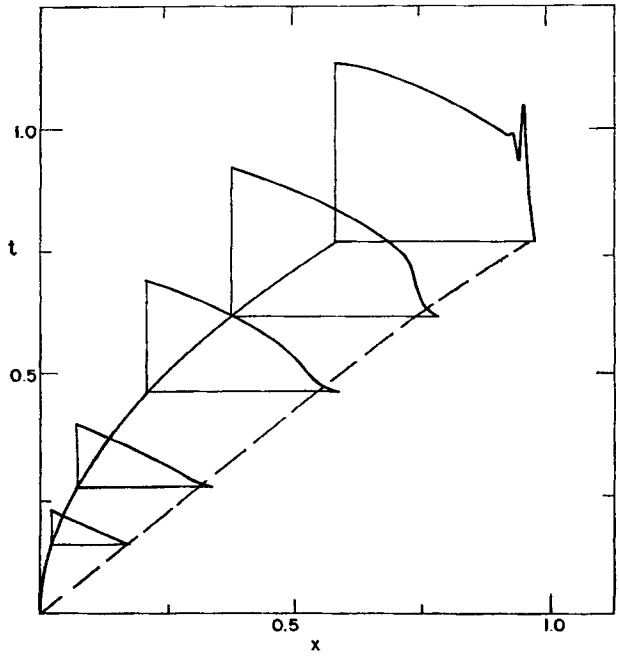

FIG. 5. Velocity distribution, viscous flow, Re = 100. Results obtained by using a constant mesh size.

in the vicinity of the first characteristic, due to the coalescence of compression waves in the inviscid case, is much weaker here. When a steady state is reached (at about $t = 1.5$), the shock thickness is very large.

In the Re = 100 case, the computation reaches a stage where compression waves, although diffused by viscosity, pile up to form a relatively thin shock. This is shown in Fig. 4, in which the shock path, as computed for inviscid flow, is denoted by a broken line. Fig. 6 again shows some of the u-distributions, compared with the u-distributions for inviscid flow. The similarity is now evident, as well as the smearing-out effect produced by viscosity in the vicinity of the shock.

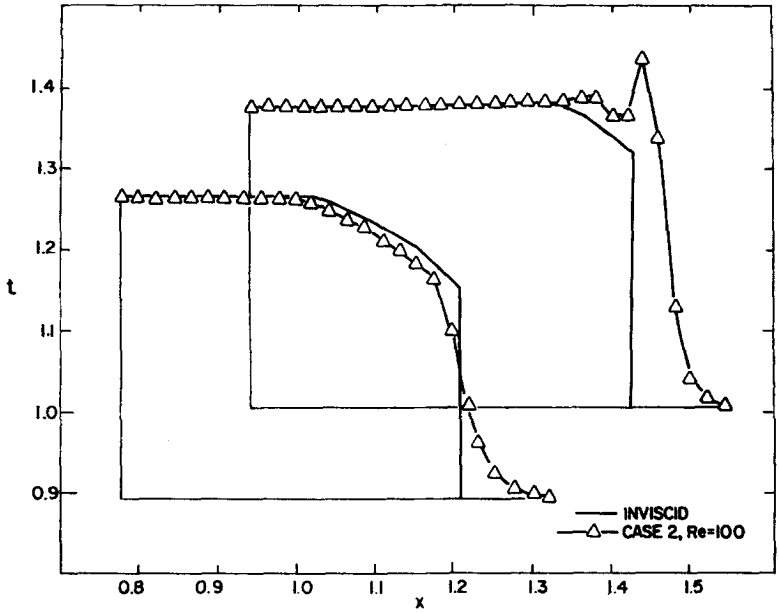

FIG. 6. Typical inviscid and viscous (Re = 100) velocity distributions.

The most interesting feature of the results appears in Fig. 4 in the plots representing $u(x)$ at $t = 0.9$ and $t = 1$. The curve tends to wrinkle in the high pressure side of the sharp transition which we will call *shock* for brevity. Oscillations appear which have the same character as in *inviscid* computations according to the available literature [2]. Such oscillations do not denote instability of the numerical scheme (they cannot be eliminated by reducing $\Delta t/\Delta x$); they denote inaccuracy. The mesh size is too wide; the truncation error, consequently, is too high [1]. In the first phase of the formation of a wiggle, first order effects are relevant; badly approximated first derivatives are not corrected sufficiently by higher order terms. The only remedy to such a situation consists of making Δx smaller.

The same effect, obviously, occurs sooner and in a stronger way if Re = 1000 (Fig. 5). Again, in Fig. 7, some comparison is made between inviscid and viscous patterns and it is obvious that viscous effects are in this case confined to a very narrow region in the vicinity of the shock but that the value of Δx is too big to provide sufficient accuracy to the computation.

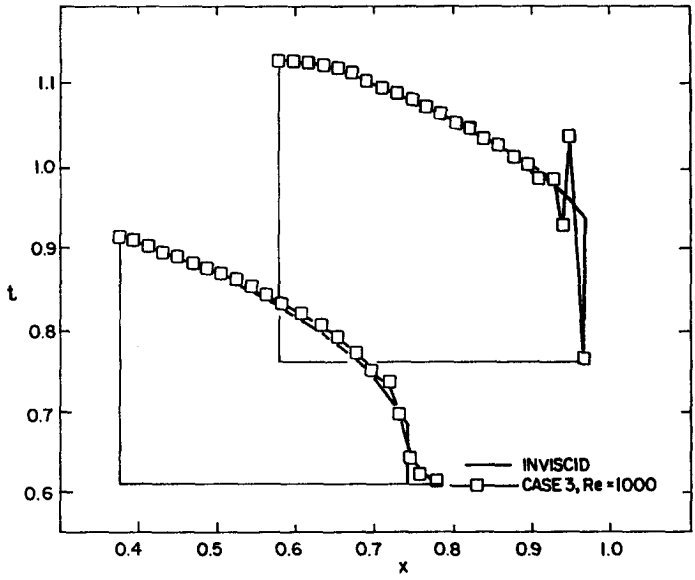

FIG. 7. Typical inviscid and viscous (Re = 1000) velocity distributions.

VI. A Second Numerical Scheme Using a Variable Mesh Size

Reducing the mesh size to values which allow sufficient accuracy at the shock may turn out to be uneconomical. For example, the value of Δx used in case 3 above should be reduced by a factor of 10; one should thus compute 10 times as many points per step and the time step size would also be reduced by a factor of 10, according to (15), so that, for the same value of t_0 as in Table I, the necessary number of steps would be multiplied by 10. The total computational time would then be multiplied by 100, rising τ to 404,500. This is indeed a terrifying value, particularly if compared with the value of τ for the inviscid computations shown in Fig. 2, which is 50. Obviously, 50 minutes of expensive machine time (at $1,200/hour) would hardly be justified by the nature of the results. A similar conclusion can be reached in two-dimensional problems, where the flow field may be not as obvious as in the present one-dimensional problem (one is, thus, disposed

to pay a certain amount of money to get the result), but where the total computational time must again be multiplied by $10M$, if M is the number of nodes in the second space direction (the price to pay becomes once more too high).

A compromise solution can be found in a variable mesh (nodes widely spaced at a distance from the shock, and clustered in the shock region). The value of Δt is still going to be small since it is controlled by the minimum value of Δx, but at least the total number of nodes should not be increased.

In planning the use of a variable mesh size, the following points have been kept in mind:

(1) The stretching of the mesh should be defined analytically so that all the additional coefficients appearing in the equations of motion in the computational space and their derivatives can be evaluated exactly at each node. This avoids the introduction of additional truncation errors in the computation.

(2) To assure a maximum value of Δt, the minimum value of Δx should be chosen at each step according to necessity and not assumed unnecessarily low. This means that the minimum value of Δx must be a function of the steepness of the transition.

(3) The minimum value of Δx should occur inside the transition.

We satisfy the conditions above as follows: Let

$$x = s(t) \tag{17}$$

be the abscissa of a certain point in the fast transition region. We will comment later on about the way of defining it as a function of time. Instead of (4), we define the change of coordinates:

$$\begin{aligned} X &= \left[Dx + \frac{\tanh \alpha(x - s)}{1.3} + E\right]\Big/2 \\ T &= t \end{aligned} \tag{18}$$

where D, E, and α are functions of t; in particular,

$$\begin{aligned} D &= 2 + \frac{\tanh \alpha(s - b - x_0) + \tanh \alpha(b - s)}{1.3x_0} \\ E &= -bD + \frac{\tanh \alpha(s - b)}{1.3} \end{aligned} \tag{19}$$

Here, x_0 is an arbitrary value, used to define the extent of the physical region to be computed; at each step the flow is evaluated between the piston (where $x = b$, $X = 0$) and the point $x = b + x_0$ (where $X = x_0$).

The transformed equations of motion are:

$$f_T + Af_X + g = 0 \tag{20}$$

where

$$A = \begin{bmatrix} C & \gamma F & 0 \\ \mathscr{T}F & C & 0 \\ 0 & 0 & C \end{bmatrix}, \qquad g = \begin{bmatrix} V_2 \\ V_1 \\ V_2 \end{bmatrix},$$

$$F = X_x, \qquad G = X_t, \qquad C = uF + G \tag{21}$$

$$V_1 = c_1(F^2 u_{XX} + F_X u_X)\,\mathscr{T}/p$$

$$V_2 = [c_2 F^2 u_X{}^2 + c_3(F^2 \mathscr{T}_{XX} + F_X \mathscr{T}_X)]/p$$

From this point on, the computation proceeds as described in section IV, with obvious modifications to the expressions of A_X and A_T.

The first condition imposed above is obviously satisfied by (18); the stretching function is defined analytically. Now, we observe that s and α are functions of t; s and α define the location of the minimum Δx and its value, respectively. Consequently, the stretching can be adjusted, in centering and strength, at every time step according to need.

In the present problem a simple way of defining α and s has been adopted. Let t_1 be the time at which the shock thickness δ, defined by

$$\delta = -\frac{u_{\text{piston}}}{(u_x)_{\max}} \tag{22}$$

becomes less than $6\Delta x$. Let $\alpha_{\max}$ be the maximum value of α, to be used when the shock is steady. The thickness Δ of the steady shock is given by (25) below. We require the minimum Δx at the steady shock to be equal to $\Delta/6$. It follows that

$$\alpha_{\max} = \frac{6}{\Delta} \tanh^{-1}(2.6\Delta X) \tag{23}$$

approximately. In addition, a time t_2 estimated at which the shock is practically steady. The estimate can be made by drawing a straight line with a slope $dx/dt = (u + a)_{\text{piston}}$ from the point at which the piston starts having a constant speed and determining its intersection with the inviscid shock path. Thus, α can be defined by

$$\alpha = \begin{cases} 0 & (t \leqslant t_1) \\ \alpha_{\max} \dfrac{t - t_1}{t_2 - t_1} & (t_1 \leqslant t \leqslant t_2) \\ \alpha_{\max} & (t \geqslant t_2) \end{cases} \tag{24}$$

In the shock region, the entropy reaches a maximum (see Section IX below). The abscissa s of such a maximum can be defined by determining the node where S is the highest and by searching for the maximum of a parabolic fit of S on that node and the two neighboring nodes. The value of s so obtained is used in (17), (18) and (19).

VII. Numerical Results, Using a Variable Mesh Size

Runs for Re = 100 and Re = 1000 were made. The pertinent values are reported in Table II, where the symbols have the same meaning as in Table I.

TABLE II

Case No.	Re	x_0	λ	α_{max}	Δx_{min}	ϵ	N	K	t_0	t_c	t_{ref}	$\tilde{t}_0$	τ
4	100	1.2	0.005	6	0.0074	0.25	61	1303	1.5	84.28″	6.6×10^{-2}	9.9×10^{-2}	850
5	1000	1.0	0.0005	60	0.00086	0.3	51	4200	1.218	256.11″	6.6×10^{-3}	8.04×10^{-3}	31903

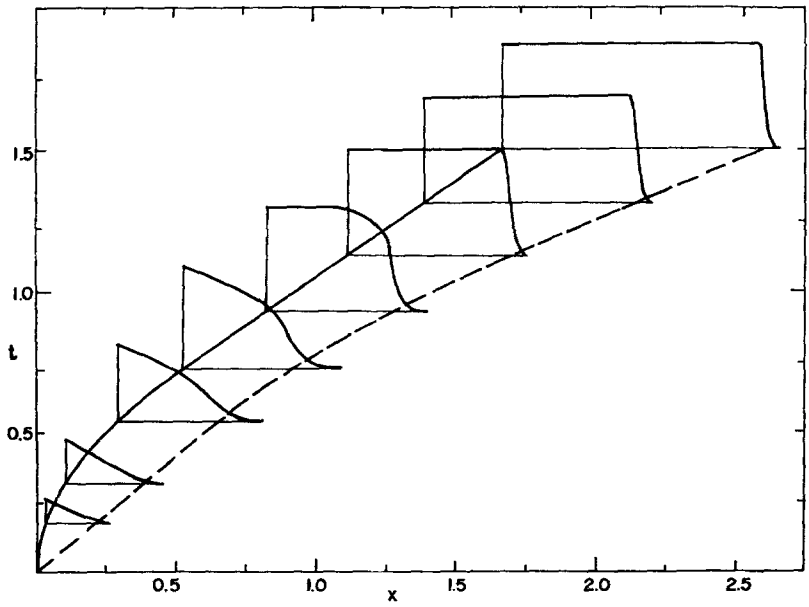

FIG. 8. Velocity distribution, viscous flow, Re = 100. Results obtained with a variable mesh.

For the case Re = 100, the computation has been carried on up to $t_0 = 1.5$, a time well beyond the one at which wiggles formed in the previous run with an even mesh. In addition, at $t = 1.5$, the inviscid flow is practically steady (Fig. 2) and we may expect that in the present viscous case a practically steady state should be reached sooner. As a matter of fact, after $t = 1.2$, there are no appreciable changes in the flow parameters in the present case. Fig. 8 shows plots of $u(x)$ at various times for Re = 100 and one can compare them to Fig. 4. Fig. 9 has the same meaning for Re = 1000; this figure can be compared with Fig. 5. Note that, in the scale of Fig. 9, the shock appears as a sharp discontinuity. Actually, there are several points with different abscissae and ordinates in the apparently vertical line (see Fig. 13 below).

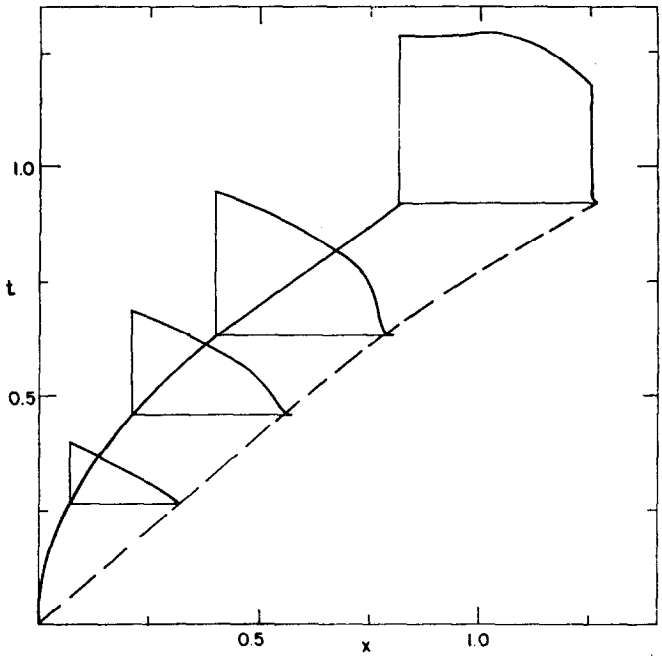

FIG. 9. Velocity distribution, viscous flow, Re = 1000. Results obtained with a variable mesh.

VIII. SHOCK WAVE THICKNESS

At this stage, the numerical scheme is submitted to the hardest test. So far, we have seen the shock build up strength and the flow behind it approach a uniform state in a way which is qualitatively satisfactory. Now, we want to make sure that

the numerical results are quantitatively correct, down to minute details of the shock wave structure.

We begin with the shock wave thickness. This is defined, as usual, as the product of the minimum value of dx/dv by the jump in v across the shock, where v is the gas velocity relative to the shock. A well-known analysis [4] shows that, for constant μ and Pr = .75,

$$\Delta = \frac{1}{\mathrm{Re}} \frac{8}{3} \frac{\gamma}{\gamma+1} \frac{1}{M} \frac{M^2-1}{1+\gamma M^2 - \sqrt{(\gamma+1)M\sqrt{2+(\gamma-1)M^2}}}$$

where M is the shock Mach number. At $M = 2$,

$$\Delta = \frac{3.24}{\mathrm{Re}} \tag{26}$$

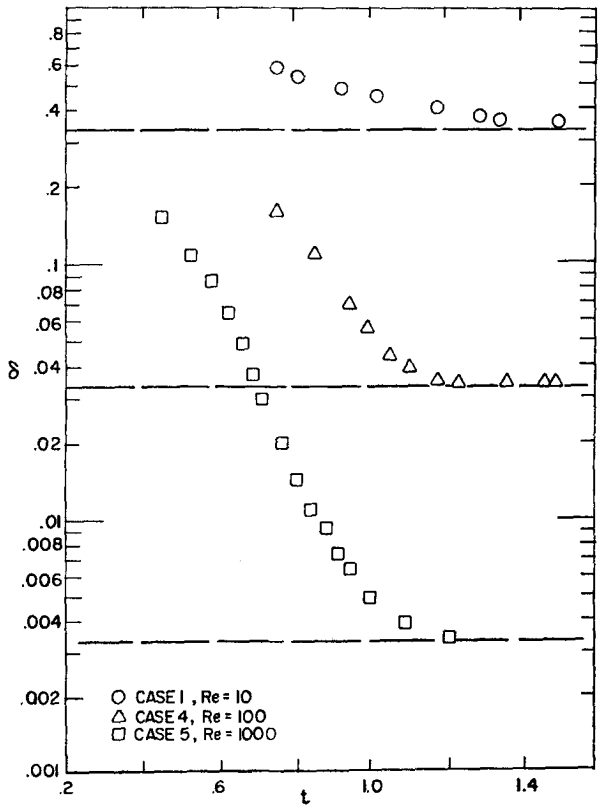

FIG. 10. Shock thickness vs. time.

The shock thicknesses resulting from the computations as functions of time are shown in Fig. 10. It is interesting to note that the shock thickness adjusts itself to the predicted value very rapidly, as soon as a steady velocity jump is reached at the shock.

IX. Entropy Distribution Across a Shock

The somewhat surprising behavior of $S(x)$ across a shock has been pointed out in [5]. Not only is the entropy higher at the high-pressure side than at the low-pressure side of the shock, as predicted by the Rankine–Hugoniot equations, but it reaches a maximum somewhere within the transitional region. The maximum is higher than the value of S at the high-pressure side of the shock.

Once more we can use this result to test our numerical computations. Three figures are presented. In Fig. 11, the maximum value of S, as computed, is shown as a function of time. It is seen that the value predicted theoretically by [5] is rapidly reached in the accelerated flow. The computed steady value agrees with the theoretical value.

Fig. 12 shows the location of points s, defined at the end of Section VI as a function of time. Since s is always contained within the shock transition, it is chosen to represent the location of the shock (in the scale of the drawing, at

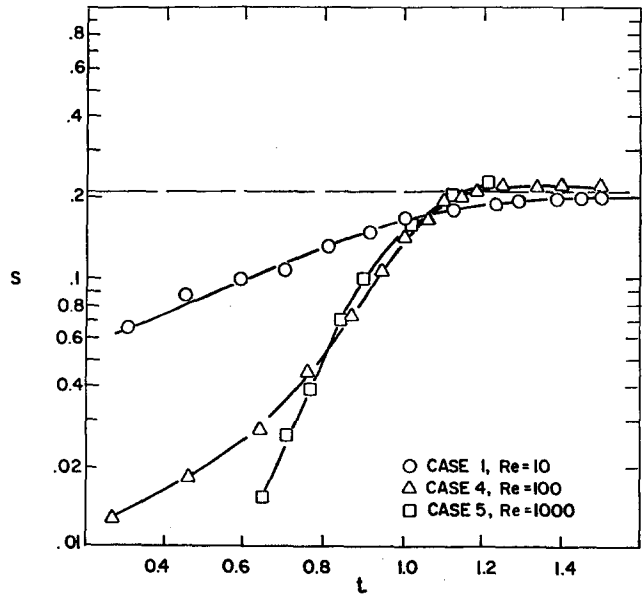

FIG. 11. Maximum value of entropy vs. time.

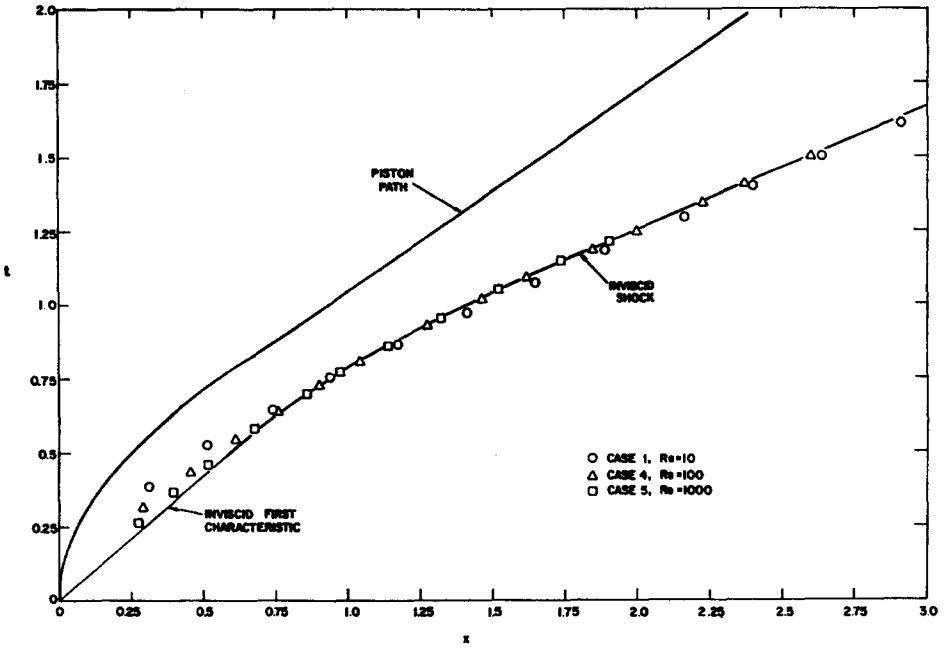

FIG. 12. Shock path.

Re = 1000, the shock has no sizable thickness). In the same figure the shock path resulting from the inviscid computation (Fig. 2) is also shown.

Finally, Fig. 13 shows, on an expanded scale, the entropy distribution across the shock as computed, in comparison with the theoretical distribution given in [5] (solid line). The agreement is good.

X. VELOCITY, PRESSURE AND TEMPERATURE DISTRIBUTIONS ACROSS A SHOCK

Fig. 13 shows also the computed distributions of velocity, pressure, and temperature across the shock, when the steady state is reached. Again, a comparison is made with the theoretical predictions of [5] (solid lines). In all cases, the agreement is very good.

XI. CONCLUSIONS

The results prove that a very accurate numerical computation of an accelerated one-dimensional viscous flow can be performed. The results show a correct depen-

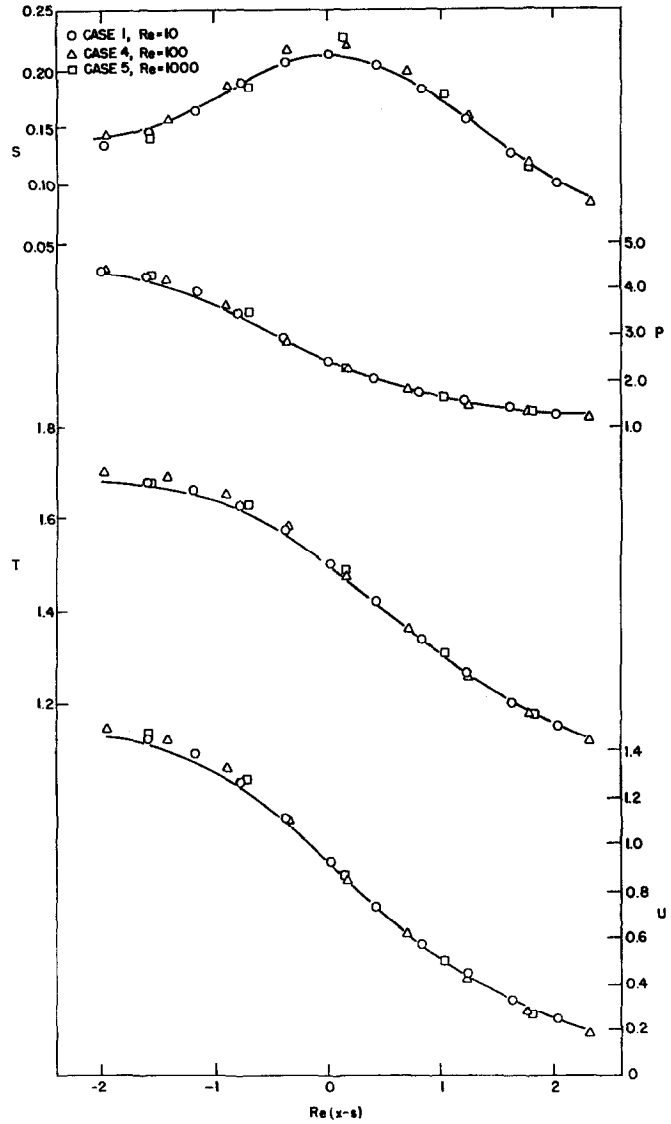

FIG. 13. Entropy, pressure, temperature, and velocity distribution across the shock.

dence on the Reynolds number. There is no interference of a spurious artificial viscosity but, instead, as Re increases, a smooth transition from the diffuse pattern, typical of low Reynolds number, to the sharp shock discontinuity, typical of inviscid flows.

In the three cases considered (Re = 10, 100, 1000, respectively), the calculation can be performed without using a prohibitive number of nodes and without exceeding reasonable limits of computational time. However, it is evident that, if a shock exists, the ratio τ between computational time and real time becomes too high if Re is of the order of 1000 or higher. For Re = 100, a sizable reduction of τ is obtained by reducing the number of nodes and increasing α accordingly. For example, if $N = 31$, $\alpha_{max} = 15$, $\Delta x_{min} = 0.0066$, a computation similar to case 4 can be performed by taking 1198 steps to a value $t_0 = 42.45$ seconds. This provides $\tau = 425$.

In conclusion, there is a lower limit for τ, and it is very high. Such a situation may be tolerable in one-dimensional problems but it makes the perspective rather bleak for two-dimensional flows. However, our results show that for Reynolds numbers of the order of 1000 or higher, *the shock thickness can be neglected* and a sharp discontinuity, satisfying the Rankine–Hugoniot conditions, can be assumed in a flow otherwise satisfying the Navier–Stokes equations. By so doing, τ is drastically reduced to values of the order of 50.

REFERENCES

1. G. MORETTI, PIBAL Report No. 69-26, Polytechnic Institute of Brooklyn, New York 11201, July, 1969.
2. G. MORETTI, PIBAL Report No. 69-25, Polytechnic Institute of Brooklyn, New York 11201, July, 1969.
3. R. COURANT, K. O. FRIEDRICHS, AND H. LEWY, *Math. Ann.* **100** (1928), 32.
4. "Modern Developments in Fluid Dynamics—High Speed Flow," (L. Howarth, Ed.), Vol. I, p. 122, Oxford Univ. Press, London/New York, 1953.
5. M. MORDUCHOW AND P. A. LIBBY, *J. Aero. Sci.* **16** (1949), 674.
6. F. D. BOYNTON AND A. THOMSON, *J. Comp. Phys.* **3** (1969), 379.